Observation of $\chi_{cJ} \to \Lambda\bar{\Lambda}\eta$

M. Ablikim,[1] M. N. Achasov,[11,b] P. Adlarson,[70] M. Albrecht,[4] R. Aliberti,[31] A. Amoroso,[69a,69c] M. R. An,[35] Q. An,[66,53] X. H. Bai,[61] Y. Bai,[52] O. Bakina,[32] R. Baldini Ferroli,[26a] I. Balossino,[27a] Y. Ban,[42,g] V. Batozskaya,[1,40] D. Becker,[31] K. Begzsuren,[29] N. Berger,[31] M. Bertani,[26a] D. Bettoni,[27a] F. Bianchi,[69a,69c] J. Bloms,[63] A. Bortone,[69a,69c] I. Boyko,[32] R. A. Briere,[5] A. Brueggemann,[63] H. Cai,[71] X. Cai,[1,53] A. Calcaterra,[26a] G. F. Cao,[1,58] N. Cao,[1,58] S. A. Cetin,[57a] J. F. Chang,[1,53] W. L. Chang,[1,58] G. Chelkov,[32,a] C. Chen,[39] Chao Chen,[50] G. Chen,[1] H. S. Chen,[1,58] M. L. Chen,[1,53] S. J. Chen,[38] S. M. Chen,[56] T. Chen,[1] X. R. Chen,[28,58] X. T. Chen,[1] Y. B. Chen,[1,53] Z. J. Chen,[23,h] W. S. Cheng,[69c] S. K. Choi,[50] X. Chu,[39] G. Cibinetto,[27a] F. Cossio,[69c] J. J. Cui,[45] H. L. Dai,[1,53] J. P. Dai,[73] A. Dbeyssi,[17] R. E. de Boer,[4] D. Dedovich,[32] Z. Y. Deng,[1] A. Denig,[31] I. Denysenko,[32] M. Destefanis,[69a,69c] F. De Mori,[69a,69c] Y. Ding,[36] J. Dong,[1,53] L. Y. Dong,[1,58] M. Y. Dong,[1,53,58] X. Dong,[71] S. X. Du,[75] P. Egorov,[32,a] Y. L. Fan,[71] J. Fang,[1,53] S. S. Fang,[1,58] W. X. Fang,[1] Y. Fang,[1] R. Farinelli,[27a] L. Fava,[69b,69c] F. Feldbauer,[4] G. Felici,[26a] C. Q. Feng,[66,53] J. H. Feng,[54] K. Fischer,[64] M. Fritsch,[4] C. Fritzsch,[63] C. D. Fu,[1] H. Gao,[58] Y. N. Gao,[42,g] Yang Gao,[66,53] S. Garbolino,[69c] I. Garzia,[27a,27b] P. T. Ge,[71] Z. W. Ge,[38] C. Geng,[54] E. M. Gersabeck,[62] A. Gilman,[64] K. Goetzen,[12] L. Gong,[36] W. X. Gong,[1,53] W. Gradl,[31] M. Greco,[69a,69c] L. M. Gu,[38] M. H. Gu,[1,53] Y. T. Gu,[14] C. Y. Guan,[1,58] A. Q. Guo,[28,58] L. B. Guo,[37] R. P. Guo,[44] Y. P. Guo,[10,f] A. Guskov,[32,a] T. T. Han,[45] W. Y. Han,[35] X. Q. Hao,[18] F. A. Harris,[60] K. K. He,[50] K. L. He,[1,58] F. H. Heinsius,[4] C. H. Heinz,[31] Y. K. Heng,[1,53,58] C. Herold,[55] M. Himmelreich,[12,d] G. Y. Hou,[1,58] Y. R. Hou,[58] Z. L. Hou,[1] H. M. Hu,[1,58] J. F. Hu,[51,i] T. Hu,[1,53,58] Y. Hu,[1] G. S. Huang,[66,53] K. X. Huang,[54] L. Q. Huang,[67] L. Q. Huang,[28,58] X. T. Huang,[45] Y. P. Huang,[1] Z. Huang,[42,g] T. Hussain,[68] N. Hüsken,[25,31] W. Imoehl,[25] M. Irshad,[66,53] J. Jackson,[25] S. Jaeger,[4] S. Janchiv,[29] E. Jang,[50] J. H. Jeong,[50] Q. Ji,[1] Q. P. Ji,[18] X. B. Ji,[1,58] X. L. Ji,[1,53] Y. Y. Ji,[45] Z. K. Jia,[66,53] H. B. Jiang,[45] S. S. Jiang,[35] X. S. Jiang,[1,53,58] Y. Jiang,[58] J. B. Jiao,[45] Z. Jiao,[21] S. Jin,[38] Y. Jin,[61] M. Q. Jing,[1,58] T. Johansson,[70] N. Kalantar-Nayestanaki,[59] X. S. Kang,[36] R. Kappert,[59] M. Kavatsyuk,[59] B. C. Ke,[75] I. K. Keshk,[4] A. Khoukaz,[63] P. Kiese,[31] R. Kiuchi,[1] R. Kliemt,[12] L. Koch,[33] O. B. Kolcu,[57a] B. Kopf,[4] M. Kuemmel,[4] M. Kuessner,[4] A. Kupsc,[40,70] W. Kühn,[33] J. J. Lane,[62] J. S. Lange,[33] P. Larin,[17] A. Lavania,[24] L. Lavezzi,[69a,69c] Z. H. Lei,[66,53] H. Leithoff,[31] M. Lellmann,[31] T. Lenz,[31] C. Li,[39] C. Li,[43] C. H. Li,[35] Cheng Li,[66,53] D. M. Li,[75] F. Li,[1,53] G. Li,[1] H. Li,[47] H. Li,[66,53] H. B. Li,[1,58] H. J. Li,[18] H. N. Li,[51,i] J. Q. Li,[4] J. S. Li,[54] J. W. Li,[45] Ke Li,[1] L. J. Li,[1] L. K. Li,[1] Lei Li,[3] M. H. Li,[39] P. R. Li,[34,j,k] S. X. Li,[10] S. Y. Li,[56] T. Li,[45] W. D. Li,[1,58] W. G. Li,[1] X. H. Li,[66,53] X. L. Li,[45] Xiaoyu Li,[1,58] H. Liang,[30] H. Liang,[66,53] H. Liang,[1,58] Y. F. Liang,[49] Y. T. Liang,[28,58] G. R. Liao,[13] L. Z. Liao,[45] J. Libby,[24] A. Limphirat,[55] C. X. Lin,[54] D. X. Lin,[28,58] T. Lin,[1] B. J. Liu,[1] C. X. Liu,[1] D. Liu,[17,66] F. H. Liu,[48] Fang Liu,[1] Feng Liu,[6] G. M. Liu,[51,i] H. Liu,[34,j,k] H. B. Liu,[14] H. M. Liu,[1,58] Huanhuan Liu,[1] Huihui Liu,[19] J. B. Liu,[66,53] J. L. Liu,[67] J. Y. Liu,[1,58] K. Liu,[1] K. Y. Liu,[36] Ke Liu,[20] L. Liu,[66,53] Lu Liu,[39] M. H. Liu,[10,f] P. L. Liu,[1] Q. Liu,[58] S. B. Liu,[66,53] T. Liu,[10,f] W. K. Liu,[39] W. M. Liu,[66,53] X. Liu,[34,j,k] Y. Liu,[34,j,k] Y. B. Liu,[39] Z. A. Liu,[1,53,58] Z. Q. Liu,[45] X. C. Lou,[1,53,58] F. X. Lu,[54] H. J. Lu,[21] J. G. Lu,[1,53] X. L. Lu,[1] Y. Lu,[7] Y. P. Lu,[1,53] Z. H. Lu,[1] C. L. Luo,[37] M. X. Luo,[74] T. Luo,[10,f] X. L. Luo,[1,53] X. R. Lyu,[58] Y. F. Lyu,[39] F. C. Ma,[36] H. L. Ma,[1] L. L. Ma,[45] M. M. Ma,[1,58] Q. M. Ma,[1] R. Q. Ma,[1,58] R. T. Ma,[58] X. Y. Ma,[1,53] Y. Ma,[42,g] F. E. Maas,[17] M. Maggiora,[69a,69c] S. Maldaner,[4] S. Malde,[64] Q. A. Malik,[68] A. Mangoni,[26b] Y. J. Mao,[42,g] Z. P. Mao,[1] S. Marcello,[69a,69c] Z. X. Meng,[61] J. G. Messchendorp,[59,12] G. Mezzadri,[27a] H. Miao,[1] T. J. Min,[38] R. E. Mitchell,[25] X. H. Mo,[1,53,58] N. Yu. Muchnoi,[11,b] Y. Nefedov,[32] F. Nerling,[17,d] I. B. Nikolaev,[11,b] Z. Ning,[1,53] S. Nisar,[9,l] Y. Niu,[45] S. L. Olsen,[58] Q. Ouyang,[1,53,58] S. Pacetti,[26b,26c] X. Pan,[10,f] Y. Pan,[52] A. Pathak,[30] M. Pelizaeus,[4] H. P. Peng,[66,53] K. Peters,[12,d] J. L. Ping,[37] R. G. Ping,[1,58] S. Plura,[31] S. Pogodin,[32] V. Prasad,[66,53] F. Z. Qi,[1] H. Qi,[66,53] H. R. Qi,[56] M. Qi,[38] T. Y. Qi,[10,f] S. Qian,[1,53] W. B. Qian,[58] Z. Qian,[54] C. F. Qiao,[58] J. J. Qin,[67] L. Q. Qin,[13] X. P. Qin,[10,f] X. S. Qin,[45] Z. H. Qin,[1,53] J. F. Qiu,[1] S. Q. Qu,[56] K. H. Rashid,[68] C. F. Redmer,[31] K. J. Ren,[35] A. Rivetti,[69c] V. Rodin,[59] M. Rolo,[69c] G. Rong,[1,58] Ch. Rosner,[17] S. N. Ruan,[39] H. S. Sang,[66] A. Sarantsev,[32,c] Y. Schelhaas,[31] C. Schnier,[4] K. Schoenning,[70] M. Scodeggio,[27a,27b] K. Y. Shan,[10,f] W. Shan,[22] X. Y. Shan,[66,53] J. F. Shangguan,[50] L. G. Shao,[1,58] M. Shao,[66,53] C. P. Shen,[10,f] H. F. Shen,[1,58] X. Y. Shen,[1,58] B. A. Shi,[58] H. C. Shi,[66,53] J. Y. Shi,[1] Q. Q. Shi,[50] R. S. Shi,[1,58] X. Shi,[1,53] X. D. Shi,[66,53] J. J. Song,[18] W. M. Song,[30,1] Y. X. Song,[42,g] S. Sosio,[69a,69c] S. Spataro,[69a,69c] F. Stieler,[31] K. X. Su,[71] P. P. Su,[50] Y. J. Su,[58] G. X. Sun,[1] H. Sun,[58] H. K. Sun,[1] J. F. Sun,[18] L. Sun,[71] S. S. Sun,[1,58] T. Sun,[1,58] W. Y. Sun,[30] X. Sun,[23,h] Y. J. Sun,[66,53] Y. Z. Sun,[1] Z. T. Sun,[45] Y. H. Tan,[71] Y. X. Tan,[66,53] C. J. Tang,[49] G. Y. Tang,[1] J. Tang,[54] L. Y. Tao,[67] Q. T. Tao,[23,h] M. Tat,[64] J. X. Teng,[66,53] V. Thoren,[70] W. H. Tian,[47] Y. Tian,[28,58] I. Uman,[57b] B. Wang,[1] B. L. Wang,[58] C. W. Wang,[38] D. Y. Wang,[42,g] F. Wang,[67] H. J. Wang,[34,j,k] H. P. Wang,[1,58] K. Wang,[1,53] L. L. Wang,[1] M. Wang,[45] M. Z. Wang,[42,g] Meng Wang,[1,58] S. Wang,[10,f] S. Wang,[13] T. Wang,[10,f] T. J. Wang,[39] W. Wang,[54] W. H. Wang,[71] W. P. Wang,[66,53] X. Wang,[42,g] X. F. Wang,[34,j,k] X. L. Wang,[10,f] Y. Wang,[56] Y. D. Wang,[41] Y. F. Wang,[1,53,58] Y. H. Wang,[43] Y. Q. Wang,[1] Yaqian Wang,[16,1] Z. Wang,[1,53] Z. Y. Wang,[1,58] Ziyi Wang,[58] D. H. Wei,[13] F. Weidner,[63] S. P. Wen,[1] D. J. White,[62] U. Wiedner,[4] G. Wilkinson,[64] M. Wolke,[70] L. Wollenberg,[4] J. F. Wu,[1,58] L. H. Wu,[1] L. J. Wu,[1,58] X. Wu,[10,f] X. H. Wu,[30] Y. Wu,[66] Y. J. Wu,[28] Z. Wu,[1,53] L. Xia,[66,53] T. Xiang,[42,g] D. Xiao,[34,j,k] G. Y. Xiao,[38] H. Xiao,[10,f] S. Y. Xiao,[1]

Y. L. Xiao,[10,f] Z. J. Xiao,[37] C. Xie,[38] X. H. Xie,[42,g] Y. Xie,[45] Y. G. Xie,[1,53] Y. H. Xie,[6] Z. P. Xie,[66,53] T. Y. Xing,[1,58] C. F. Xu,[1] C. J. Xu,[54] G. F. Xu,[1] H. Y. Xu,[61] Q. J. Xu,[15] X. P. Xu,[50] Y. C. Xu,[58] Z. P. Xu,[38] F. Yan,[10,f] L. Yan,[10,f] W. B. Yan,[66,53] W. C. Yan,[75] H. J. Yang,[46,e] H. L. Yang,[30] H. X. Yang,[1] L. Yang,[47] S. L. Yang,[58] Tao Yang,[1] Y. F. Yang,[39] Y. X. Yang,[1,58] Yifan Yang,[1,58] M. Ye,[1,53] M. H. Ye,[8] J. H. Yin,[1] Z. Y. You,[54] B. X. Yu,[1,53,58] C. X. Yu,[39] G. Yu,[1,58] T. Yu,[67] C. Z. Yuan,[1,58] L. Yuan,[2] S. C. Yuan,[1] X. Q. Yuan,[1] Y. Yuan,[1,58] Z. Y. Yuan,[54] C. X. Yue,[35] A. A. Zafar,[68] F. R. Zeng,[45] X. Zeng,[6] Y. Zeng,[23,h] Y. J. Zeng,[39] Y. H. Zhan,[54] A. Q. Zhang,[1] B. L. Zhang,[1] B. X. Zhang,[1] D. H. Zhang,[39] G. Y. Zhang,[18] H. Zhang,[66] H. H. Zhang,[54] H. H. Zhang,[30] H. Y. Zhang,[1,53] J. L. Zhang,[72] J. Q. Zhang,[37] J. W. Zhang,[1,53,58] J. X. Zhang,[34,j,k] J. Y. Zhang,[1] J. Z. Zhang,[1,58] Jianyu Zhang,[1,58] Jiawei Zhang,[1,58] L. M. Zhang,[56] L. Q. Zhang,[54] Lei Zhang,[38] P. Zhang,[1] Q. Y. Zhang,[35,75] Shuihan Zhang,[1,58] Shulei Zhang,[23,h] X. D. Zhang,[41] X. M. Zhang,[1] X. Y. Zhang,[45] X. Y. Zhang,[50] Y. Zhang,[64] Y. T. Zhang,[75] Y. H. Zhang,[1,53] Yan Zhang,[66,53] Yao Zhang,[1] Z. H. Zhang,[1] Z. Y. Zhang,[39] Z. Y. Zhang,[71] G. Zhao,[1] J. Zhao,[35] J. Y. Zhao,[1,58] J. Z. Zhao,[1,53] Lei Zhao,[66,53] Ling Zhao,[1] M. G. Zhao,[39] Q. Zhao,[1] S. J. Zhao,[75] Y. B. Zhao,[1,53] Y. X. Zhao,[28,58] Z. G. Zhao,[66,53] A. Zhemchugov,[32,a] B. Zheng,[67] J. P. Zheng,[1,53] Y. H. Zheng,[58] B. Zhong,[37] C. Zhong,[67] X. Zhong,[54] H. Zhou,[45] L. P. Zhou,[1,58] X. Zhou,[71] X. K. Zhou,[58] X. R. Zhou,[66,53] X. Y. Zhou,[35] Y. Z. Zhou,[10,f] J. Zhu,[39] K. Zhu,[1] K. J. Zhu,[1,53,58] L. X. Zhu,[58] S. H. Zhu,[65] S. Q. Zhu,[38] T. J. Zhu,[72] W. J. Zhu,[10,f] Y. C. Zhu,[66,53] Z. A. Zhu,[1,58] B. S. Zou,[1] and J. H. Zou[1]

(BESIII Collaboration)

[1]*Institute of High Energy Physics, Beijing 100049, People's Republic of China*
[2]*Beihang University, Beijing 100191, People's Republic of China*
[3]*Beijing Institute of Petrochemical Technology, Beijing 102617, People's Republic of China*
[4]*Bochum Ruhr-University, D-44780 Bochum, Germany*
[5]*Carnegie Mellon University, Pittsburgh, Pennsylvania 15213, USA*
[6]*Central China Normal University, Wuhan 430079, People's Republic of China*
[7]*Central South University, Changsha 410083, People's Republic of China*
[8]*China Center of Advanced Science and Technology, Beijing 100190, People's Republic of China*
[9]*COMSATS University Islamabad, Lahore Campus, Defence Road, Off Raiwind Road, 54000 Lahore, Pakistan*
[10]*Fudan University, Shanghai 200433, People's Republic of China*
[11]*G.I. Budker Institute of Nuclear Physics SB RAS (BINP), Novosibirsk 630090, Russia*
[12]*GSI Helmholtzcentre for Heavy Ion Research GmbH, D-64291 Darmstadt, Germany*
[13]*Guangxi Normal University, Guilin 541004, People's Republic of China*
[14]*Guangxi University, Nanning 530004, People's Republic of China*
[15]*Hangzhou Normal University, Hangzhou 310036, People's Republic of China*
[16]*Hebei University, Baoding 071002, People's Republic of China*
[17]*Helmholtz Institute Mainz, Staudinger Weg 18, D-55099 Mainz, Germany*
[18]*Henan Normal University, Xinxiang 453007, People's Republic of China*
[19]*Henan University of Science and Technology, Luoyang 471003, People's Republic of China*
[20]*Henan University of Technology, Zhengzhou 450001, People's Republic of China*
[21]*Huangshan College, Huangshan 245000, People's Republic of China*
[22]*Hunan Normal University, Changsha 410081, People's Republic of China*
[23]*Hunan University, Changsha 410082, People's Republic of China*
[24]*Indian Institute of Technology Madras, Chennai 600036, India*
[25]*Indiana University, Bloomington, Indiana 47405, USA*
[26a]*INFN Laboratori Nazionali di Frascati, I-00044, Frascati, Italy*
[26b]*INFN Sezione di Perugia, I-06100, Perugia, Italy*
[26c]*University of Perugia, I-06100, Perugia, Italy*
[27a]*INFN Sezione di Ferrara, I-44122, Ferrara, Italy*
[27b]*University of Ferrara, I-44122, Ferrara, Italy*
[28]*Institute of Modern Physics, Lanzhou 730000, People's Republic of China*
[29]*Institute of Physics and Technology, Peace Avenue 54B, Ulaanbaatar 13330, Mongolia*
[30]*Jilin University, Changchun 130012, People's Republic of China*
[31]*Johannes Gutenberg University of Mainz, Johann-Joachim-Becher-Weg 45, D-55099 Mainz, Germany*
[32]*Joint Institute for Nuclear Research, 141980 Dubna, Moscow region, Russia*
[33]*Justus-Liebig-Universitaet Giessen, II. Physikalisches Institut, Heinrich-Buff-Ring 16, D-35392 Giessen, Germany*
[34]*Lanzhou University, Lanzhou 730000, People's Republic of China*
[35]*Liaoning Normal University, Dalian 116029, People's Republic of China*

[36]Liaoning University, Shenyang 110036, People's Republic of China
[37]Nanjing Normal University, Nanjing 210023, People's Republic of China
[38]Nanjing University, Nanjing 210093, People's Republic of China
[39]Nankai University, Tianjin 300071, People's Republic of China
[40]National Centre for Nuclear Research, Warsaw 02-093, Poland
[41]North China Electric Power University, Beijing 102206, People's Republic of China
[42]Peking University, Beijing 100871, People's Republic of China
[43]Qufu Normal University, Qufu 273165, People's Republic of China
[44]Shandong Normal University, Jinan 250014, People's Republic of China
[45]Shandong University, Jinan 250100, People's Republic of China
[46]Shanghai Jiao Tong University, Shanghai 200240, People's Republic of China
[47]Shanxi Normal University, Linfen 041004, People's Republic of China
[48]Shanxi University, Taiyuan 030006, People's Republic of China
[49]Sichuan University, Chengdu 610064, People's Republic of China
[50]Soochow University, Suzhou 215006, People's Republic of China
[51]South China Normal University, Guangzhou 510006, People's Republic of China
[52]Southeast University, Nanjing 211100, People's Republic of China
[53]State Key Laboratory of Particle Detection and Electronics, Beijing 100049, Hefei 230026, People's Republic of China
[54]Sun Yat-Sen University, Guangzhou 510275, People's Republic of China
[55]Suranaree University of Technology, University Avenue 111, Nakhon Ratchasima 30000, Thailand
[56]Tsinghua University, Beijing 100084, People's Republic of China
[57a]Turkish Accelerator Center Particle Factory Group, Istinye University, 34010, Istanbul, Turkey
[57b]Near East University, Nicosia, North Cyprus, Mersin 10, Turkey
[58]University of Chinese Academy of Sciences, Beijing 100049, People's Republic of China
[59]University of Groningen, NL-9747 AA Groningen, The Netherlands
[60]University of Hawaii, Honolulu, Hawaii 96822, USA
[61]University of Jinan, Jinan 250022, People's Republic of China
[62]University of Manchester, Oxford Road, Manchester, M13 9PL, United Kingdom
[63]University of Muenster, Wilhelm-Klemm-Strasse 9, 48149 Muenster, Germany
[64]University of Oxford, Keble Road, Oxford OX13RH, United Kingdom
[65]University of Science and Technology Liaoning, Anshan 114051, People's Republic of China
[66]University of Science and Technology of China, Hefei 230026, People's Republic of China
[67]University of South China, Hengyang 421001, People's Republic of China
[68]University of the Punjab, Lahore-54590, Pakistan
[69a]University of Turin and INFN, University of Turin, I-10125, Turin, Italy
[69b]University of Eastern Piedmont, I-15121, Alessandria, Italy
[69c]INFN, I-10125, Turin, Italy
[70]Uppsala University, Box 516, SE-75120 Uppsala, Sweden
[71]Wuhan University, Wuhan 430072, People's Republic of China
[72]Xinyang Normal University, Xinyang 464000, People's Republic of China
[73]Yunnan University, Kunming 650500, People's Republic of China
[74]Zhejiang University, Hangzhou 310027, People's Republic of China
[75]Zhengzhou University, Zhengzhou 450001, People's Republic of China

[a]Also at the Moscow Institute of Physics and Technology, Moscow 141700, Russia.
[b]Also at the Novosibirsk State University, Novosibirsk, 630090, Russia.
[c]Also at the NRC "Kurchatov Institute," PNPI, 188300, Gatchina, Russia.
[d]Also at Goethe University Frankfurt, 60323 Frankfurt am Main, Germany.
[e]Also at Key Laboratory for Particle Physics, Astrophysics and Cosmology, Ministry of Education; Shanghai Key Laboratory for Particle Physics and Cosmology; Institute of Nuclear and Particle Physics, Shanghai 200240, People's Republic of China.
[f]Also at Key Laboratory of Nuclear Physics and Ion-beam Application (MOE) and Institute of Modern Physics, Fudan University, Shanghai 200443, People's Republic of China.
[g]Also at State Key Laboratory of Nuclear Physics and Technology, Peking University, Beijing 100871, People's Republic of China.
[h]Also at School of Physics and Electronics, Hunan University, Changsha 410082, China.
[i]Also at Guangdong Provincial Key Laboratory of Nuclear Science, Institute of Quantum Matter, South China Normal University, Guangzhou 510006, China.
[j]Also at Frontiers Science Center for Rare Isotopes, Lanzhou University, Lanzhou 730000, People's Republic of China.
[k]Also at Lanzhou Center for Theoretical Physics, Lanzhou University, Lanzhou 730000, People's Republic of China.
[l]Also at the Department of Mathematical Sciences, IBA, Karachi, Pakistan.

(Received 24 June 2022; accepted 15 September 2022; published 14 October 2022)

By analyzing $(448.1 \pm 2.9) \times 10^6$ $\psi(3686)$ events collected with the BESIII detector operating at the BEPCII collider, the decays of $\chi_{cJ} \to \Lambda\bar{\Lambda}\eta$ ($J = 0$, 1, and 2) are observed for the first time with statistical significances of 13.9σ, 6.7σ, and 8.2σ, respectively. The product branching fractions of $\psi(3686) \to \gamma\chi_{cJ}$ and $\chi_{cJ} \to \Lambda\bar{\Lambda}\eta$ are measured. Dividing by the world averages of the branching fractions of $\psi(3686) \to \gamma\chi_{cJ}$, the branching fractions of $\chi_{cJ} \to \Lambda\bar{\Lambda}\eta$ decays are determined to be $(2.31 \pm 0.30 \pm 0.21) \times 10^{-4}$, $(5.86 \pm 1.38 \pm 0.68) \times 10^{-5}$, and $(1.05 \pm 0.21 \pm 0.15) \times 10^{-4}$ for $J = 0$, 1 and 2, respectively, where the first uncertainties are statistical and the second systematic.

DOI: 10.1103/PhysRevD.106.072004

I. INTRODUCTION

Studies of the processes involving $B\bar{B}P$, where B and P denote baryons and pseudoscalar mesons, respectively, are important to search for possible $B\bar{B}$ threshold enhancements and excited baryon states decaying into BP. An enhancement around the $\Lambda\bar{\Lambda}$ production threshold was observed in the $e^+e^- \to \phi\Lambda\bar{\Lambda}$ process [1], and the interpretation of $\Lambda\bar{\Lambda}$ enhancement originating from decay of the $\eta(2225) \to \Lambda\bar{\Lambda}$ [2] was rejected with a significance of 7σ. Similar structure was also reported in the B meson decays $B^0 \to \Lambda\bar{\Lambda}K^0$ and $B^+ \to \Lambda\bar{\Lambda}K^+$ [3]. On the other hand, an excited Λ state, $\Lambda(1670)$, was observed in the $\Lambda\eta$ mass spectra in the near-threshold reaction $K^-p \to \eta\Lambda$ [4] and the charmonium decay $\psi(3686) \to \Lambda\bar{\Lambda}\eta$ [5]. However, experimental results on the $\Lambda\bar{\Lambda}$ production threshold enhancement and on excited Λ states decaying into $\Lambda\eta$ are still limited. Comprehensive investigations of the $B\bar{B}P$ system in the various charmonium state decays are desirable. To date, only a few studies of $\chi_{cJ} \to B\bar{B}P$ ($J = 0$, 1, 2) have been performed [6], and no investigation of $\chi_{cJ} \to \Lambda\bar{\Lambda}\eta$ has been reported. Observation of $\chi_{cJ} \to \Lambda\bar{\Lambda}\eta$ would provide an opportunity to better understand the enhancement around the $\Lambda\bar{\Lambda}$ production threshold and a possible excited Λ state, e.g., $\Lambda(1670)$.

In the quark model, the χ_{cJ} mesons are identified as ^3P_J charmonium states. Because of parity conservation, they cannot be produced by e^+e^- annihilation directly. As a result, the decays of χ_{cJ} have not been studied as extensively as the vector charmonium states J/ψ and $\psi(3686)$ in both experiment and theory. However, the radiative decays of $\psi(3686)$ into χ_{cJ} mesons have branching fractions of about 9% [6] for each χ_{cJ} state, thereby offering an ideal testbed to investigate χ_{cJ} meson decays.

In this paper, by analyzing $(448.1 \pm 2.9) \times 10^6$ $\psi(3686)$ events [7] collected with the BESIII detector [8], we present the first measurements of the branching fractions of χ_{cJ} decays to $\Lambda\bar{\Lambda}\eta$.

II. BESIII DETECTOR AND MONTE CARLO SIMULATION

The BESIII detector is a magnetic spectrometer [8] located at the Beijing Electron Positron Collider (BEPCII) [9]. The cylindrical core of the BESIII detector consists of a main drift chamber filled with helium-based gas, a plastic scintillator time-of-flight system (TOF), and a CsI(Tl) electromagnetic calorimeter (EMC), which are all enclosed in a superconducting solenoidal magnet providing a 1.0 T magnetic field. The flux-return yoke is instrumented with resistive plate chambers arranged in nine layers in the barrel and eight layers in the end caps for muon identification. The acceptance of charged particles and photons is 93% of 4π solid angle. The charged-particle momentum resolution at 1.0 GeV/c is 0.5%, and the specific energy loss resolution is 6% for the electrons from Bhabha scattering. The EMC measures photon energies with a resolution of 2.5% (5%) at 1 GeV in the barrel (end cap) region. The time resolution of the TOF barrel part is 68 ps, while that of the end cap part is 110 ps.

Simulated samples produced with the GEANT4-based [10] Monte Carlo (MC) software, which includes the geometric description of the BESIII detector and the detector response, are used to determine the detection efficiencies and to estimate the background levels. The simulation takes into account the beam energy spread and initial state radiation in the e^+e^- annihilation modeled with the generator KKMC [11]. The inclusive MC samples consist of 5.06×10^8 $\psi(3686)$ events, the initial state radiation production of the J/ψ state, and the continuum processes incorporated in KKMC. The known decay modes are modeled with EVTGEN [12] using the branching fractions taken from the Particle Data Group [6], and the remaining unknown decays from the charmonium states with LUNDCHARM [13]. Final state radiation is incorporated with PHOTOS [14].

For each signal process of $\psi(3686) \to \gamma\chi_{cJ}, \chi_{cJ} \to \Lambda\bar{\Lambda}\eta$, $\Lambda(\bar{\Lambda}) \to p\pi^-(\bar{p}\pi^+)$, 5×10^5 signal MC events are generated. Radiative decay $\psi(3686) \to \gamma\chi_{cJ}$ is generated with a $1 + \lambda\cos^2\theta$ distribution, where θ is the angle between the direction of the radiative photon and the beam, and $\lambda = 1, -1/3, 1/13$ for $J = 0, 1, 2$ [12] in accordance with expectations for electric dipole transitions. Intrinsic width and mass values as given in Ref. [6] are used for the χ_{cJ} states in the simulation. The process of $\chi_{cJ} \to \Lambda\bar{\Lambda}\eta$ is simulated with the BODY3 generator based on EVTGEN [12], as discussed in Sec. V. The decay of $\Lambda(\bar{\Lambda}) \to p\pi^-(\bar{p}\pi^+)$ is simulated in phase space.

III. EVENT SELECTION

In this analysis, the Λ, $\bar{\Lambda}$, and η particles are reconstructed via the $\Lambda \to p\pi^-$, $\bar{\Lambda} \to \bar{p}\pi^+$, and $\eta \to \gamma\gamma$ decays, respectively.

All charged tracks are required to satisfy $|Z_v| < 20$ cm and $|\cos\theta| < 0.93$, where Z_v denotes the distance from the interaction point to the point of closest approach of the reconstructed track to the z axis, which is the symmetry axis of the main drift chamber, and θ is the polar angle relative to the z axis. Candidate events must have four charged tracks with zero net charge and at least three good photons. The $\Lambda(\bar{\Lambda})$ candidates are reconstructed using vertex fits of all oppositely charged track pairs, which are assumed to be $p\pi^-(\bar{p}\pi^+)$ without particle identification. To suppress the $p\pi^-(\bar{p}\pi^+)$ combinatorial background, the reconstructed decay lengths of the $\Lambda(\bar{\Lambda})$ candidates are required to be more than twice their standard deviations. Figure 1 shows the distributions of $M_{p\pi^-}$ and $M_{p\pi^-}$ versus $M_{\bar{p}\pi^+}$ of survived candidates in data. The invariant mass of $p\pi^-(\bar{p}\pi^+)$ is required to be within the $\Lambda(\bar{\Lambda})$ signal region, defined as $|M_{p\pi^-(\bar{p}\pi^+)} - m_{\Lambda(\bar{\Lambda})}| < 6$ MeV/c^2, where $m_{\Lambda(\bar{\Lambda})}$ is the $\Lambda(\bar{\Lambda})$ nominal mass [6], while the one-dimensional (1D) $\Lambda(\bar{\Lambda})$ sideband region is defined as $10 < |M_{p\pi^-(\bar{p}\pi^+)} - m_{\Lambda(\bar{\Lambda})}| < 22$ MeV/c^2. The two-dimensional (2D) $\Lambda\bar{\Lambda}$ signal region is defined as the square region with both $p\pi^-$ and $\bar{p}\pi^+$ combinations lying in the $\Lambda(\bar{\Lambda})$ signal regions. The $\Lambda\bar{\Lambda}$ sideband I regions are defined as the square regions with either one of the $p\pi^-$ or $\bar{p}\pi^+$ combinations locating in the 1D $\Lambda(\bar{\Lambda})$ sideband regions and the other in the 1D signal region. The sideband II regions are defined as the square regions with both $p\pi^-$ and $\bar{p}\pi^+$ combinations locating in the 1D $\Lambda(\bar{\Lambda})$ sideband regions.

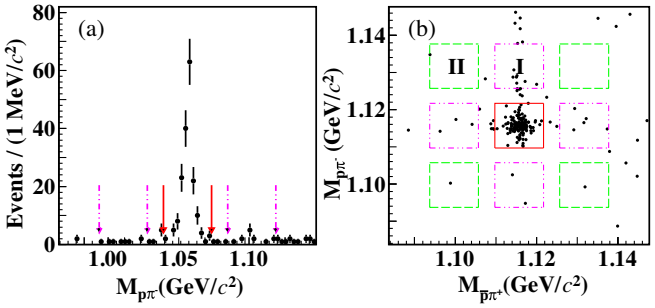

FIG. 1. The distributions of (a) $M_{p\pi^-}$ and (b) $M_{p\pi^-}$ versus $M_{\bar{p}\pi^+}$ of the candidates for $\psi(3686) \to \gamma\chi_{cJ}$ with $\chi_{cJ} \to \Lambda\bar{\Lambda}\eta$ in data, where all requirements except for the $\Lambda(\bar{\Lambda})$ signal region have been imposed. In (a), the pair of red solid arrows denote the Λ signal region, and the pairs of pink dot-dashed arrows denote sideband regions of the accepted candidates. In (b), the red solid rectangle denotes the $\Lambda\bar{\Lambda}$ signal region, the pink dot-dashed rectangles denote the $\Lambda\bar{\Lambda}$ sideband I region, and the green dashed rectangles denote the $\Lambda\bar{\Lambda}$ sideband II region.

Good photon candidates are chosen from isolated clusters in the EMC. Their energies are required to be greater than 25 MeV in the barrel ($|\cos\theta| < 0.8$) and 50 MeV in the end cap ($0.86 < |\cos\theta| < 0.92$) regions. Reconstructed clusters due to electronic noise or beam backgrounds are suppressed by requiring the timing information to be within [0, 700] ns after the event start time. To suppress fake photons produced by hadronic interactions in the EMC and secondary photons from bremsstrahlung, clusters within a cone angle of 20° around the extrapolated position in the EMC of any charged track are rejected. The energy deposited in the neighbor TOF counters is taken into account to improve the reconstruction efficiency and energy resolution.

To further suppress the combinatorial background, a four-momentum conservation constraint (4C) kinematic fit under the hypothesis of $e^+e^- \to \Lambda\bar{\Lambda}\gamma\gamma\gamma$ is applied to the events. The combination with the minimum $\chi^2_{\rm 4C}$ is kept for further analysis. The $\chi^2_{\rm 4C}$ of the kinematic fit is required to be less than 50 based on optimization with the Punzi significance method [15] with the formula $\frac{\epsilon}{1.5+\sqrt{B}}$, where ϵ is the detection efficiency and B is the number of background events from the inclusive $\psi(3686)$ MC sample. This requirement will reject 84% of background and lose 14% of signal efficiency.

The three selected photons are ordered according to their energies with $E_{\gamma_1} > E_{\gamma_2} > E_{\gamma_3}$, defined as γ_1, γ_2, and γ_3. The η candidates are reconstructed from either $\gamma_1\gamma_2$ or $\gamma_1\gamma_3$ pair. Based on MC study, excluding η candidates from $\gamma_2\gamma_3$ could suppress the background by 6% with the signal efficiency loss less than 0.1%, and improves the Punzi significance by 3%. Figure 2 shows the $M_{\gamma\gamma}$ distribution of η candidates of the accepted events in data. The η signal and sideband regions are defined as $|M_{\gamma\gamma} - 0.54| < 0.04$ GeV/c^2 and $0.08 < |M_{\gamma\gamma} - 0.54| < 0.12$ GeV/c^2, respectively. Events with both $M_{\gamma_1\gamma_2}$ and $M_{\gamma_1\gamma_3}$ being in the η signal region are excluded from analysis. Events with neither $M_{\gamma_1\gamma_2}$ or $M_{\gamma_1\gamma_3}$ within the signal region, but either $M_{\gamma_1\gamma_2}$ or $M_{\gamma_1\gamma_3}$ in the sideband region, are taken as sideband events.

To suppress background events associated with $J/\psi \to \Lambda\bar{\Lambda}\gamma$, events with $|M_{\Lambda\bar{\Lambda}\gamma_{1,2,3}} - 3.101| < 0.044$ GeV/c^2 are

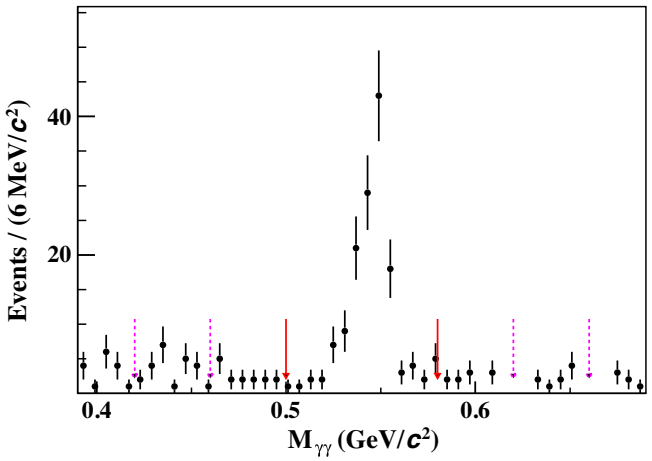

FIG. 2. The $M_{\gamma\gamma}$ distribution of η candidates of the accepted events in data. The pair of red solid arrows denote the η signal region and the pairs of pink dot-dashed arrows denote the η sideband regions.

vetoed, where the veto region is five standard deviations of the resolution around the mean value. To suppress background events related to $\chi_{cJ} \to \Lambda\bar{\Lambda}\pi^0$, events with $|M_{\gamma\gamma} - 0.137| < 0.015$ GeV/c^2 are excluded for all three possible photon pairs. To suppress background events associated with $\Sigma(\bar{\Sigma}) \to \Lambda(\bar{\Lambda})\gamma$, events with $|M_{\Lambda(\bar{\Lambda})\gamma_{2,3}} - 1.192| < 0.015$ GeV/c^2 are rejected.

A total of 144 candidate events survive from all requirements. Figure 3(a) shows the distribution of $M_{\Lambda\bar{\Lambda}\eta}$ of the accepted candidate events in data. Clear signals of χ_{c0}, χ_{c1}, and χ_{c2} are observed. The distributions of $M_{\Lambda\bar{\Lambda}}$, $M_{\Lambda\eta}$, and $M_{\bar{\Lambda}\eta}$ from all χ_{cJ} signal regions of the data sample are shown in Fig. 4. Here, the signal regions of χ_{c0}, χ_{c1}, and χ_{c2} are defined as [3.385, 3.445], [3.490, 3.530], and [3.536, 3.576] GeV/c^2, respectively. With present statistics, it is impossible to conclude that there is an enhancement near the $\Lambda\bar{\Lambda}$ production threshold in Fig. 4(a). In addition, no obvious excited Λ state is found in Figs. 4(b) or 4(c). Meanwhile, we can not conclude whether there is any structure difference between the $M_{\Lambda\bar{\Lambda}}$, $M_{\Lambda\eta}$, and $M_{\bar{\Lambda}\eta}$ spectra from different χ_{cJ} signal regions.

IV. BACKGROUND STUDIES

Possible non-$\Lambda(\bar{\Lambda})$ background and non-η peaking background from $\psi(3686)$ decays are studied with sideband events. Figures 3(b) and 3(c) show the $M_{\Lambda\bar{\Lambda}\eta}$ distributions of candidate events in the $\Lambda\bar{\Lambda}$ sideband I region and η sideband region, respectively. No significant non-$\Lambda(\bar{\Lambda})$ peaking background and non-η peaking background is observed. For the $\Lambda\bar{\Lambda}$ sideband II region, only three events are remained, which are negligible.

Potential backgrounds with $\Lambda\bar{\Lambda}\eta + X$ final states are estimated by analyzing the inclusive $\psi(3686)$ MC sample with TopoAna [16]. No peaking background is found except for $\chi_{c2} \to \Sigma^0\bar{\Lambda}\eta$. However, the $\chi_{c2} \to \Sigma^0\bar{\Lambda}\eta$ decay is an isospin-violating process and no branching fraction is available. The yield of this background is estimated by assuming that the ratio $\frac{\mathcal{B}(\chi_{c2}\to\Sigma^0\bar{\Lambda}\eta)}{\mathcal{B}(\chi_{c2}\to\Lambda\bar{\Lambda}\eta)}$ is comparable with $\frac{\mathcal{B}(J/\psi\to\Sigma^0\bar{\Lambda})}{\mathcal{B}(J/\psi\to\Lambda\bar{\Lambda})} = 1.5\%$ or $\frac{\mathcal{B}(\psi(3686)\to\Sigma^0\bar{\Lambda})}{\mathcal{B}(\psi(3686)\to\Lambda\bar{\Lambda})} = 3.2\%$ [6] based on isospin symmetry. MC studies show that the ratio of the yield of this background relative to our signal is less than 0.1%. Therefore this background is also negligible in this analysis.

Finally, the possible quantum electrodynamics (QED) contribution is examined by using the continuum data corresponding to an integrated luminosity of 44.45 pb^{-1} taken at the center-of-mass energy of 3.65 GeV [17]. No event survives the selection criteria. Therefore, the QED contribution is also neglected in this analysis.

V. BRANCHING FRACTIONS

To determine signal yields, an unbinned maximum likelihood fit is performed on the $M_{\Lambda\bar{\Lambda}\eta}$ distribution of the accepted candidates in data. In the fit, the χ_{cJ} signals are

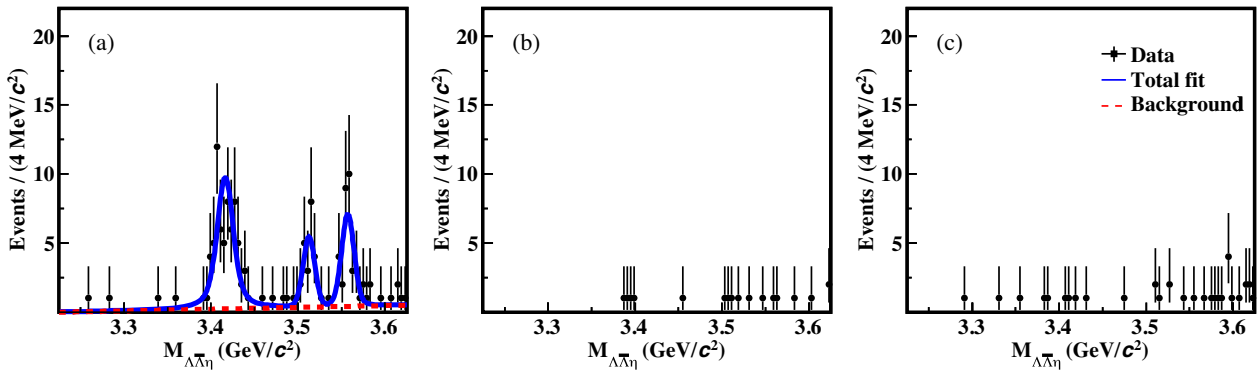

FIG. 3. The $M_{\Lambda\bar{\Lambda}\eta}$ distributions of the accepted events in (a) the combined $\Lambda\bar{\Lambda}$ and η signal region, (b) the $\Lambda\bar{\Lambda}$ sideband I region, and (c) the η sideband region. The points with error bars are data, the red dashed curve is the fitted background shape, and the blue solid curve is the overall fit.

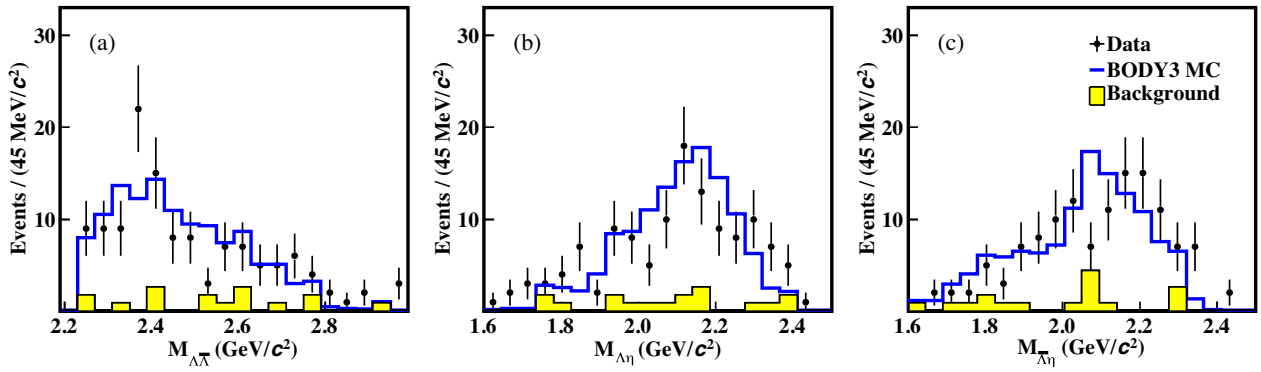

FIG. 4. The distributions of (a) $M_{\Lambda\bar{\Lambda}}$, (b) $M_{\Lambda\eta}$, and (c) $M_{\bar{\Lambda}\eta}$ from the three χ_{cJ} signal regions of the data sample. The points with error bars are data. The blue solid curves are BODY3 MC events. The yellow filled histograms are the simulated backgrounds. The signal and background yields have been normalized to the statistics of data.

described with individual Breit-Wigner functions $\frac{1}{(M_{\Lambda\bar{\Lambda}\eta}-m_{\chi_{cJ}})^2+\Gamma^2_{\chi_{cJ}}/4}$ convolved with a Gaussian function. The masses and widths of Breit-Wigner functions are fixed to their world average values [6]. The mean and width of the Gaussian function are free parameters. Because the potential peaking background is negligible, a linear function is chosen to describe the combinatorial background shape. For each signal decay mode, the statistical significance is calculated with $\Delta(\ln\mathcal{L}) = \ln\mathcal{L}_{\rm max} - \ln\mathcal{L}_0$ and $\Delta ndf = 3$. Here, the $\mathcal{L}_{\rm max}$ and $\mathcal{L}_0$ are the maximum likelihoods with and without the signal component in the fits; the Δndf is the variation of number of degrees of freedom. The statistical significances are 13.7σ, 6.2σ, and 7.7σ for $\chi_{c0} \to \Lambda\bar{\Lambda}\eta$, $\chi_{c1} \to \Lambda\bar{\Lambda}\eta$, and $\chi_{c2} \to \Lambda\bar{\Lambda}\eta$, respectively. As shown in Fig. 3(a), we obtain the signal yields of χ_{c0}, χ_{c1}, and χ_{c2} to be 66.9 ± 8.8, 21.3 ± 5.0, and 31.6 ± 6.2, respectively, where the uncertainties are statistical only.

The $\chi_{cJ} \to \Lambda\bar{\Lambda}\eta$ decays are simulated with a modified data-driven generator BODY3, which was developed to simulate different intermediate states in data for a given three-body final state. Initially, a phase space MC sample is used to determine efficiency over the whole allowed kinematic region. Then, the Dalitz plot of $M^2_{\Lambda\eta}$ versus $M^2_{\bar{\Lambda}\eta}$, corrected for backgrounds and efficiencies, is used to determine the probability of an event configuration generated randomly. The detection efficiencies for $\psi(3686) \to \gamma\chi_{c0,1,2}$ with $\chi_{c0,1,2} \to \Lambda\bar{\Lambda}\eta$ are $(4.11 \pm 0.03)\%$, $(5.17 \pm 0.03)\%$, and $(4.37 \pm 0.03)\%$, respectively, where the errors are statistical only.

The product branching fractions of $\psi(3686) \to \gamma\chi_{cJ}$ and $\chi_{cJ} \to \Lambda\bar{\Lambda}\eta$ are calculated with

$$\mathcal{B}(\psi(3686) \to \gamma\chi_{cJ}) \cdot \mathcal{B}(\chi_{cJ} \to \Lambda\bar{\Lambda}\eta) = \frac{N^J_{\rm obs}}{N_{\psi(3686)} \cdot \mathcal{B}^2(\Lambda \to p\pi^-) \cdot \mathcal{B}(\eta \to \gamma\gamma) \cdot \epsilon(\chi_{cJ} \to \Lambda\bar{\Lambda}\eta)}, \quad (1)$$

where $N^J_{\rm obs}$ is the signal yield obtained from the fit to the $M_{\Lambda\bar{\Lambda}\eta}$ distribution for χ_{cJ}, $N_{\psi(3686)} = (448.1 \pm 2.9) \times 10^6$ is the number of $\psi(3686)$ events [7], $\epsilon(\chi_{cJ} \to \Lambda\bar{\Lambda}\eta)$ is the detection efficiency for χ_{cJ}, and $\mathcal{B}(\Lambda \to p\pi^-)$ and $\mathcal{B}(\eta \to \gamma\gamma)$ are the branching fractions of $\Lambda \to p\pi^-$ and $\eta \to \gamma\gamma$ from Ref. [6]. Dividing by the world averages [6] of $\mathcal{B}(\psi(3686) \to \gamma\chi_{c0}) = (9.79 \pm 0.20)\%$, $\mathcal{B}(\psi(3686) \to \gamma\chi_{c1}) = (9.75 \pm 0.24)\%$, and $\mathcal{B}(\psi(3686) \to \gamma\chi_{c2}) = (9.52 \pm 0.20)\%$, we obtain the branching fractions of $\chi_{cJ} \to \Lambda\bar{\Lambda}\eta$ decays. The obtained results are summarized in Table I.

VI. SYSTEMATIC UNCERTAINTIES

The systematic uncertainties in the branching fraction measurements, described below, come from several sources, as summarized in Table II.

TABLE I. Signal yields in data, detection efficiencies, and the branching fractions $\mathcal{B}(\psi(3686) \to \gamma\chi_{cJ})$, $\mathcal{B}(\psi(3686) \to \gamma\chi_{cJ}) \cdot \mathcal{B}(\chi_{cJ} \to \Lambda\bar{\Lambda}\eta)$, and $\mathcal{B}(\chi_{cJ} \to \Lambda\bar{\Lambda}\eta)$. The first errors are statistical and the second systematic.

	χ_{c0}	χ_{c1}	χ_{c2}
$N^J_{\rm obs}$	66.9 ± 8.8	21.3 ± 5.0	31.6 ± 6.2
$\epsilon(\chi_{cJ} \to \Lambda\bar{\Lambda}\eta)$	$(4.11 \pm 0.03)\%$	$(5.17 \pm 0.03)\%$	$(4.37 \pm 0.03)\%$
$\mathcal{B}(\psi(3686) \to \gamma\chi_{cJ}) \cdot \mathcal{B}(\chi_{cJ} \to \Lambda\bar{\Lambda}\eta)$	$(2.26 \pm 0.30 \pm 0.20) \times 10^{-5}$	$(5.72 \pm 1.34 \pm 0.65) \times 10^{-6}$	$(1.00 \pm 0.20 \pm 0.14) \times 10^{-5}$
$\mathcal{B}(\psi(3686) \to \gamma\chi_{cJ})$ [6]	$(9.79 \pm 0.20)\%$	$(9.75 \pm 0.24)\%$	$(9.52 \pm 0.20)\%$
$\mathcal{B}(\chi_{cJ} \to \Lambda\bar{\Lambda}\eta)$	$(2.31 \pm 0.30 \pm 0.21) \times 10^{-4}$	$(5.87 \pm 1.38 \pm 0.68) \times 10^{-5}$	$(1.05 \pm 0.21 \pm 0.15) \times 10^{-4}$

TABLE II. Relative systematic uncertainties (%) in the measurements of the branching fractions of $\chi_{cJ} \to \Lambda\bar{\Lambda}\eta$.

Source	χ_{c0}	χ_{c1}	χ_{c2}
$N_{\psi(3686)}$	0.7	0.7	0.7
$\Lambda(\bar{\Lambda})$ reconstruction	1.8	5.2	5.7
γ selection	3.0	3.0	3.0
η mass window	1.0	1.0	1.0
Rejection of $J/\psi \to \Lambda\bar{\Lambda}\gamma$	...	0.9	8.1
Rejection of $\chi_{cJ} \to \Lambda\bar{\Lambda}\pi^0$	...	1.8	2.9
Rejection of $\Sigma(\bar{\Sigma})$	...	6.3	4.5
$M_{\Lambda\bar{\Lambda}\eta}$ fit	6.8	4.0	2.1
BODY3 generator	3.2	4.7	7.5
4C kinematic fit	2.0	2.3	2.8
MC statistics	0.7	0.6	0.6
$\mathcal{B}(\psi(3686) \to \gamma\chi_{cJ})$	2.0	2.5	2.1
$\mathcal{B}(\Lambda \to p\pi^-)$	1.6	1.6	1.6
$\mathcal{B}(\eta \to \gamma\gamma)$	0.5	0.5	0.5
Total	9.0	11.6	14.6

The systematic uncertainty of the $\psi(3686)$ event number $N_{\psi(3686)}$ is 0.7% [7].

The efficiencies of $\Lambda(\bar{\Lambda})$ reconstruction, including the tracking efficiencies of the $p\pi^-(\bar{p}\pi^+)$ pair, decay length requirement, mass window requirement, vertex fit, and second vertex fit, are studied using the control samples of $J/\psi \to pK^-\bar{\Lambda} + \text{c.c.}$ and $J/\psi \to \Lambda\bar{\Lambda}$. The efficiency difference between data and MC simulation $\Delta\epsilon^i = \epsilon_i^{\text{data}}/\epsilon_i^{\text{MC}} - 1$ in each momentum and $\cos\theta$ bin of data is weighted by $w_i = \frac{N_i}{N_{\text{tot}}}$, where N_i is the number of generated MC events in the ith bin and N_{tot} is the total number of generated MC events. The differences of the detection efficiencies between data and MC simulation $\sum w_i \times \Delta\epsilon^i$ are assigned as the corresponding systematic uncertainties, which are 1.6%, 2.9%, and 3.0% for Λ and 0.2%, 2.3%, and 2.7% for $\bar{\Lambda}$ in $\chi_{c0} \to \Lambda\bar{\Lambda}\eta$, $\chi_{c1} \to \Lambda\bar{\Lambda}\eta$, and $\chi_{c2} \to \Lambda\bar{\Lambda}\eta$, respectively.

The systematic uncertainty due to the photon detection is determined to be 1.0% per photon by using the control sample $J/\psi \to \pi^+\pi^-\pi^0$ [18].

The systematic uncertainty related to the η mass window is studied with the control sample of $\psi(3686) \to \eta J/\psi$, $J/\psi \to l^+l^-$ ($l = e, \mu$). The difference of the acceptance efficiencies between data and MC simulation, 1.0%, is taken to be the corresponding systematic uncertainty.

The systematic uncertainties arising from rejections of $J/\psi \to \Lambda\bar{\Lambda}\gamma$, $\chi_{cJ} \to \Lambda\bar{\Lambda}\pi^0$, and $\Sigma(\bar{\Sigma}) \to \Lambda(\bar{\Lambda})\gamma$ are estimated by varying individual rejection windows by one time of resolutions in $M_{\Lambda\bar{\Lambda}\gamma}$, $M_{\gamma\gamma}$, and $M_{\Lambda(\bar{\Lambda})\gamma}$, respectively. Totally 1000 pseudodatasets are sampled with replacement data for each case according to the bootstrap method [19]. For each pseudodataset, similar fit is performed on $M_{\Lambda\bar{\Lambda}\eta}$ as the fit to real data. We examine the pull distribution relative to the fit yield of real data, which is

$$p(N_{\text{sig}}) = \frac{N_{\text{sig}}^{\text{pseudo}} - N_{\text{sig}}^{\text{real}}}{\sigma_{N_{\text{sig}}^{\text{pseudo}}}}, \tag{2}$$

where $N_{\text{sig}}^{\text{real}}$ is the fit yield of real data, and $N_{\text{sig}}^{\text{pseudo}}$ and $\sigma_{N_{\text{sig}}^{\text{pseudo}}}$ are the fit yield and its statistical uncertainty of pseudodata, respectively. We fit to this pull distribution with a Gaussian function. If the mean value is greater than two times of its standard deviation, the maximum deviation will be assigned as the corresponding systematic uncertainty. The systematic uncertainties due to $J/\psi \to \Lambda\bar{\Lambda}\gamma$, $\chi_{cJ} \to \Lambda\bar{\Lambda}\pi^0$, and $\Sigma(\bar{\Sigma}) \to \Lambda(\bar{\Lambda})\gamma$ rejections are assigned to be 0.9%, 1.8%, and 6.3% for $\chi_{c1} \to \Lambda\bar{\Lambda}\eta$; and 8.1%, 2.9%, and 4.5% for $\chi_{c2} \to \Lambda\bar{\Lambda}\eta$, respectively; while those for $\chi_{c0} \to \Lambda\bar{\Lambda}\eta$ are negligible with deviation less than 2σ.

The systematic uncertainties in the $M_{\Lambda\bar{\Lambda}\eta}$ fit are considered in two aspects. The systematic uncertainties associated with the signal shape are estimated by using alternative signal shapes based on MC simulation. The changes of the fitted signal yields, 2.2%, 2.3%, and 1.9% for $\chi_{c0} \to \Lambda\bar{\Lambda}\eta$, $\chi_{c1} \to \Lambda\bar{\Lambda}\eta$, and $\chi_{c2} \to \Lambda\bar{\Lambda}\eta$, respectively, are taken as the corresponding systematic uncertainties. The systematic uncertainties from the background shape are estimated by using a second order polynomial. The changes of the fitted signal yields, 6.4%, 3.3%, and 1.0% for $\chi_{c0} \to \Lambda\bar{\Lambda}\eta$, $\chi_{c1} \to \Lambda\bar{\Lambda}\eta$, and $\chi_{c2} \to \Lambda\bar{\Lambda}\eta$, respectively, are taken as the corresponding systematic uncertainties. Adding them in quadrature, we obtain the systematic uncertainties due to the $M_{\Lambda\bar{\Lambda}\eta}$ fit to be 6.8%, 4.0%, and 2.1% for $\chi_{c0} \to \Lambda\bar{\Lambda}\eta$, $\chi_{c1} \to \Lambda\bar{\Lambda}\eta$, and $\chi_{c2} \to \Lambda\bar{\Lambda}\eta$, respectively.

The systematic uncertainty due to the BODY3 generator is estimated by varying the weight in each bin by $\pm 1\sigma$. The weights in various bins are obtained with data after subtracting the normalized background from inclusive $\psi(3686)$ MC sample. The change of the weighted signal efficiency caused by each bin is obtained to be $\Delta\epsilon_i$. Summing $\Delta\epsilon_i$ over all bins with $\sqrt{\sum_{i=1}^{n_{\text{bin}}} \Delta\epsilon_i^2}$, the associated systematic uncertainties are obtained to be 3.4%, 4.7%, and 7.5% for $\chi_{c0} \to \Lambda\bar{\Lambda}\eta$, $\chi_{c1} \to \Lambda\bar{\Lambda}\eta$, and $\chi_{c2} \to \Lambda\bar{\Lambda}\eta$, respectively.

The systematic uncertainties of the 4C kinematic fit are assigned as the differences between the detection efficiencies before and after the helix parameter corrections [20], which are 2.0% for $\chi_{c0} \to \Lambda\bar{\Lambda}\eta$, 2.3% for $\chi_{c1} \to \Lambda\bar{\Lambda}\eta$, and 2.8% for $\chi_{c2} \to \Lambda\bar{\Lambda}\eta$.

The uncertainties due to the limited MC statistics are calculated from $\sqrt{\frac{1-\epsilon}{N\cdot\epsilon}}$, where ϵ is the detection efficiency and N is the number of signal MC events. They are 0.7%, 0.6%, and 0.6% for $\chi_{c0} \to \Lambda\bar{\Lambda}\eta$, $\chi_{c1} \to \Lambda\bar{\Lambda}\eta$, and $\chi_{c2} \to \Lambda\bar{\Lambda}\eta$, respectively.

The uncertainties from the world averages of the branching fractions of $\psi(3686) \to \gamma\chi_{c0}$, $\psi(3686) \to \gamma\chi_{c1}$,

$\psi(3686) \to \gamma\chi_{c2}$, $\Lambda \to p\pi^-$, and $\eta \to \gamma\gamma$ [6] are 2.0%, 2.5%, 2.1%, 0.8%, and 0.5%, respectively.

For each signal decay, the total systematic uncertainty is calculated by adding systematic uncertainties quadratically under the assumption that all sources are independent.

VII. SUMMARY

By analyzing $(448.1 \pm 2.9) \times 10^6$ $\psi(3686)$ events collected with the BESIII detector, we observe the decays of $\chi_{c0,1,2} \to \Lambda\bar{\Lambda}\eta$ for the first time. The product branching fractions of $\psi(3686) \to \gamma\chi_{cJ}$ and $\chi_{cJ} \to \Lambda\bar{\Lambda}\eta$ are determined. Dividing by the world averages of the branching fractions of $\psi(3686) \to \gamma\chi_{cJ}$, we determine the branching fractions of $\chi_{cJ} \to \Lambda\bar{\Lambda}\eta$ as summarized in Table I. The current available statistics is not sufficient to draw any conclusion that there is an enhancement near the $\Lambda\bar{\Lambda}$ production. We look at the $M_{\Lambda\eta}$ or $M_{\bar{\Lambda}\eta}$ spectra and do not find any excited Λ state.

ACKNOWLEDGMENTS

The BESIII collaboration thanks the staff of BEPCII and the IHEP computing center for their strong support. This work is supported in part by National Key R&D Program of China under Grants No. 2020YFA0406300 and No. 2020YFA0406400; National Natural Science Foundation of China (NSFC) under Grants No. 12035009, No. 11875170, No. 11475090, No. 11635010, No. 11735014, No. 11835012, No. 11935015, No. 11935016, No. 11935018, No. 11961141012, No. 12022510, No. 12025502, No. 12035013, No. 12192260, No. 12192261, No. 12192262, No. 12192263, No. 12192264, and No. 12192265; the Chinese Academy of Sciences (CAS) Large-Scale Scientific Facility Program; Joint Large-Scale Scientific Facility Funds of the NSFC and CAS under Grant No. U1832207; CAS Key Research Program of Frontier Sciences under Grant No. QYZDJ-SSW-SLH040; 100 Talents Program of CAS; The Institute of Nuclear and Particle Physics (INPAC) and Shanghai Key Laboratory for Particle Physics and Cosmology; ERC under Grant No. 758462; European Union's Horizon 2020 research and innovation program under Marie Sklodowska-Curie grant agreement under Grant No. 894790; German Research Foundation DFG under Grant No. 443159800, Collaborative Research Center CRC 1044, GRK 2149; Istituto Nazionale di Fisica Nucleare, Italy; Ministry of Development of Turkey under Grant No. DPT2006K-120470; National Science and Technology fund; National Science Research and Innovation Fund (NSRF) via the Program Management Unit for Human Resources & Institutional Development, Research and Innovation under Grant No. B16F640076; STFC (United Kingdom); Suranaree University of Technology (SUT), Thailand Science Research and Innovation (TSRI), and National Science Research and Innovation Fund (NSRF) under Grant No. 160355; The Royal Society, UK under Grants No. DH140054 and No. DH160214; The Swedish Research Council; U.S. Department of Energy under Grant No. DE-FG02-05ER41374.

[1] M. Ablikim *et al.* (BESIII Collaboration), Phys. Rev. D **104**, 052006 (2021).
[2] L. Zhao, N. Li, S. L. Zhu, and B. S. Zou, Phys. Rev. D **87**, 054034 (2013).
[3] Y. W. Chang *et al.* (Belle Collaboration), Phys. Rev. D **79**, 052006 (2009).
[4] D. M. Manley *et al.* (Crystal Ball Collaboration), Phys. Rev. Lett. **88**, 012002 (2001).
[5] M. Ablikim *et al.* (BESIII Collaboration), Phys. Rev. D **87**, 052007 (2013).
[6] R. L. Workman *et al.* (Particle Data Group), Prog. Theor. Exp. Phys. **2022**, 083C01 (2022).
[7] M. Ablikim *et al.* (BESIII Collaboration), Chin. Phys. C **42**, 023001 (2018).
[8] M. Ablikim *et al.* (BESIII Collaboration), Nucl. Instrum. Methods Phys. Res., Sect. A **614**, 345 (2010).
[9] C. H. Yu *et al.*, *Proceedings of the 7th International Particle Accelerator Conference* (JACoW, Geneva, Switzerland, 2016), p. TUYA01, https://accelconf.web.cern.ch/ipac2016/doi/JACoW-IPAC2016-TUYA01.html.
[10] S. Agostinelli *et al.* (GEANT4 Collaboration), Nucl. Instrum. Methods Phys. Res., Sect. A **506**, 250 (2003).
[11] S. Jadach, B. F. L. Ward, and Z. Was, Phys. Rev. D **63**, 113009 (2001).
[12] D. J. Lange, Nucl. Instrum. Methods Phys. Res., Sect. A **462**, 152 (2001); R. G. Ping, Chin. Phys. C **32**, 599 (2008).
[13] J. C. Chen, G. S. Huang, X. R. Qi, D. H. Zhang, and Y. S. Zhu, Phys. Rev. D **62**, 034003 (2000).
[14] E. Richter-Was, Phys. Lett. B **303**, 163 (1993).
[15] G. Punzi, arXiv:2011.11770.
[16] X. Y. Zhou, S. X. Du, G. Li, and C. P. Shen, Comput. Phys. Commun. **258**, 107540 (2021).
[17] M. Ablikim *et al.* (BESIII Collaboration), Chin. Phys. C **37**, 123001 (2013).
[18] M. Ablikim *et al.* (BESIII Collaboration), Phys. Rev. D **86**, 052011 (2012).
[19] B. Efron, Ann. Stat. **7**, 1 (1979).
[20] M. Ablikim *et al.* (BESIII Collaboration), Phys. Rev. D **87**, 012002 (2013).